ELSEVIER

Journal of Nuclear Materials 280 (2000) 304–311

journal of nuclear materials

www.elsevier.nl/locate/jnucmat

Crack growth pattern and threshold stress intensity factor, K_{IH}, of Zr–2.5Nb alloy with the notch direction

Young Suk Kim *, Sang Chul Kwon, Sung Soo Kim

Zirconium Team, Korea Atomic Energy Research Institute, P.O. Box 105, Yusong, Taejon 305-600, South Korea

Received 18 October 1999; accepted 6 April 2000

Abstract

The objective of this study is to obtain a better understanding of the threshold stress intensity factor for an initiation of delayed hydride cracking (DHC) in a Zr–2.5Nb pressure tube. By changing the crack propagation from the longitudinal direction to the circumferential direction, the threshold stress intensity factor, K_{IH}, and the crack growth pattern were investigated in the Zr–2.5Nb pressure tube with a strong circumferential texture. The threshold stress intensity factor, K_{IH}, was discussed phenomenologically based on the crack growth pattern and analytically as a function of the tilting angle of hydride habit planes to the cracking plane. A supplementary experiment was conducted to demonstrate a linear decrease of K_{IH} with an increase in the basal pole component in the cracking plane. Thus, it is concluded that the DHC is controlled by the nucleation and growth of the hydride precipitates on the habit plane.

PACS: 62.20.MK

1. Introduction

Zr–2.5 wt% Nb (or Zr–2.5Nb) pressure tubes used in CANDU nuclear power plants are very susceptible to delayed hydride cracking (DHC) due to the hydrogen pick up during its operation [1,2]. Therefore, there is a strong incentive to increase the DHC resistance of Zr–2.5Nb alloy. A current understanding of the DHC phenomenon is that the DHC crack always grows normal to the direction of applied stress by fracturing of hydrides reoriented ahead of the crack tip [3–5]. However, it may not always be true when the hydride habit plane is not in accordance with the cracking plane. Since the crack grows by fracturing of hydrides, an initiation of the DHC crack would depend strongly on the orientation of the hydride habit plane where the hydrides preferentially can precipitate. In other words, if the hydride habit plane is parallel to the cracking plane, the DHC crack initiation will be easy. On the contrary, where the hydride habit plane is tilting from the cracking plane, the crack initiation will be difficult, leading to an increase in threshold stress intensity factor, K_{IH}, or to an increase in DHC resistance.

Since $\{10\bar{1}7\}$ planes are the most favorable habit planes for the precipitation of hydrides in zirconium alloys under tensile stress [6], the initiation of DHC may depend strongly on the available number of the habit planes that is determined by texture. In other words, K_{IH} may depend on how many habit planes are lying parallel to the cracking plane or on the angle between them, or on texture in short. The aim of this study is to obtain a better understanding of the DHC phenomenon, finding a way to increase the threshold stress intensity factor, K_{IH}. To clearly investigate a dependence of crack initiation and propagation with texture, flattened compact tension (CT) specimens were subjected to a constant tensile load with the fatigue cracking plane varying from the longitudinal direction to the transverse one of the Zr–2.5Nb pressure tube with a strong circumferential texture.

* Corresponding author. Tel.: +82-42 868 2359; fax: +82-42 868 8346.

E-mail address: yskiml@kaeri.re.kr (Y.S. Kim).

0022-3115/00/$ - see front matter
PII: S0022-3115(00)00054-4

2. Experimental procedure

The Zr–2.5Nb pressure tube with a strong circumferential texture was subjected to flattening by a press into a sheet of around 4.0 mm thick followed by a vacuum annealing treatment at 400°C for 48 h to relieve residual stress. CT specimens were made in accordance with ASTM E-399-83. To investigate the texture effect on the DHC, the notch direction changed from the longitudinal direction to the circumferential one as shown in Fig. 1. We have used four kinds of CT specimens such as L0, L30, L45 and L90 where the number next to L represents the angle between the notch direction and the longitudinal direction of the pressure tube. All the specimens were subjected to charging of hydrogen to 200 ± 20 ppm by using Sievert's equipment followed by a homogenizing treatment at 400°C for 24 h in 10^{-5} torr. Details of the Sievert's equipment were described in [7]. Fatigue cracks were made by using an lnstron machine (Model no. 8562) with a stress intensity factor of 12 MPa $\sqrt{m}$ at the beginning which was reduced to 7 MPa $\sqrt{m}$ finally along with the propagation of the crack [8]. CT specimens were subjected to a constant load in tension in a creep machine while the initiation and growth of the crack were monitored by a dc potential drop method. The applied load of 4 MPa $\sqrt{m}$ initially was applied during heating up to 300°C, soaking at 300°C for 1 h and cooling down to 200°C [8,9]. The crack propagation was checked through an increasing load stepwise from 7 to 30 MPa $\sqrt{m}$. After the crack grew by 0.5 to 2 mm, the specimens were heat tinted at 300°C for 1 h. The crack velocity was derived from the average crack depth divided by the time over which steady cracking proceeded [4]. The crack profile was observed to measure the crack growth direction at the side surface of each specimen.

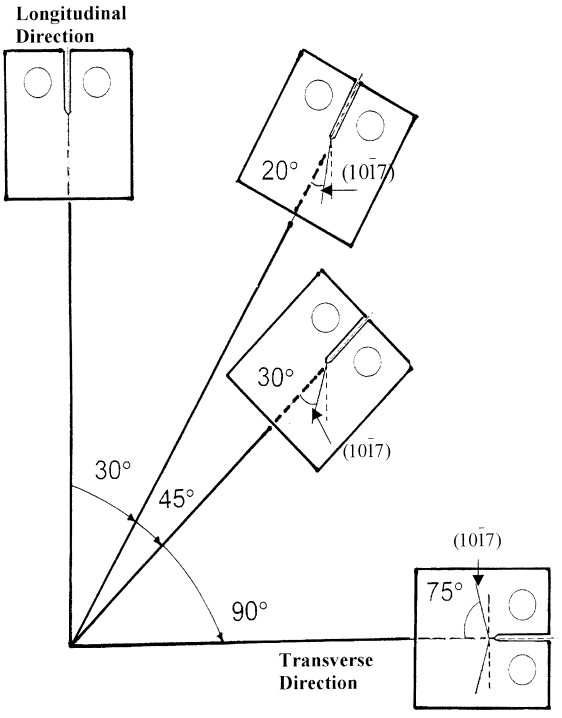

Fig. 1. Compact tension specimens with a notch slanted at various angles to the longitudinal direction.

3. Results and discussion

3.1. Crack growth pattern and K_{IH} on the notch orientation

Fig. 2 shows typical DHC crack growth patterns observed on the four kinds of CT specimens. As expected, L0 CT specimen had the crack growing along the notch direction that is normal to the tensile stress. In contrast, neither L30 nor L45 specimens had the crack growth along the notch direction, but they showed slanted cracks at some angles to the tensile load direction. Even though a U type groove with 0.6 mm deep and 0.1 mm root radius was made on either side of the specimen to facilitate the crack growing in the direction normal to the applied stress as shown in Fig. 3(a), the crack did not grow straight along the groove but tilted toward the longitudinal direction as shown in Fig. 3(b). This explicitly demonstrates that the DHC crack grows along a habit plane somehow. The angle of the slanted crack to the longitudinal direction was found to be 15° for both of them. Furthermore, L90 specimen had a crack branching where an angle between the branched cracks corresponded to 150°. In other words, the branched cracks were directed towards the longitudinal direction of the pressure tube as seen on L30 or L45 specimens. Table 1 summarized the measured tilting angles of the DHC crack and the initial notch plane or the longitudinal direction of the pressure tube, respectively. One thing to note is that tilting of the cracking plane to the longitudinal direction is consistently equal to about 15° except for the L0 specimen.

The Zr–2.5Nb pressure tube used for this study has shown a strong circumferential texture where the majority of the (0 0 0 1) basal pole aligns in the circumferential direction as shown in Fig. 4 and Table 2. The longitudinal direction and the radial direction are parallel to the poles of (1 0 $\bar{1}$ 0) plane and (1 1 $\bar{2}$ 0) plane, respectively. Since hydrides precipitate on the habit planes (1 0 $\bar{1}$ 7) under tensile stress [6,10], and the crack grows by hydrides precipitated on the habit planes, the cracking plane will be tilted at 15° from the basal plane (0 0 0 2). This is well consistent with our observation on the DHC crack growth pattern shown in Fig. 2 except for the L0 specimen.

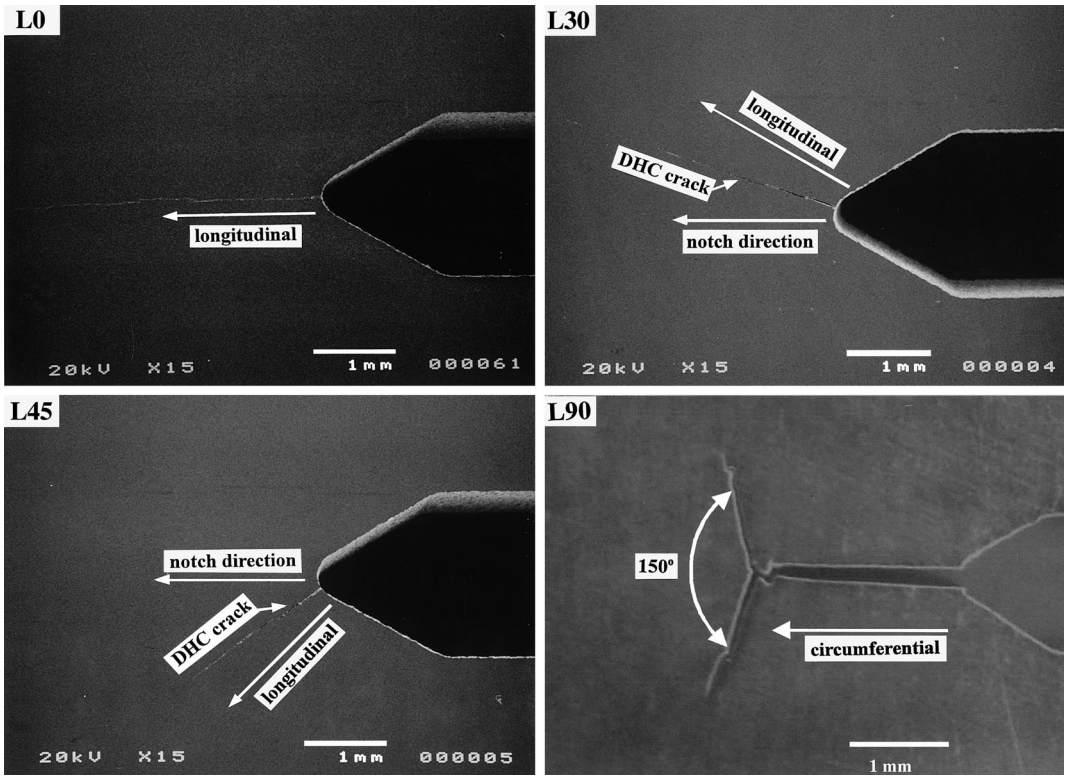

Fig. 2. Crack growth pattern observed on four kinds of CT specimens: straight crack for L0, slanted crack for L30 or L45 and a crack branching for L90.

For L90 specimen, the directions of the notch and the applied stress correspond with $\langle 0\,0\,0\,2\rangle$ and $\langle 1\,0\,\bar{1}\,0\rangle$, respectively while the habit planes, $(1\,0\,\bar{1}\,7)$ and $(\bar{1}\,0\,1\,7)$, lie symmetrically $\pm 75°$ to the notch direction as shown in Fig. 5(a). Since the stress conditions on the two symmetric planes are equal, the nucleation and growth of hydrides would proceed along the two planes, leading to the crack branching with an angle of 150° as shown in Fig. 2. This kind of crack slanting had also been reported very roughly by Coleman [11] and Huang and Mills [12]. L30 specimen has the two habit planes, $(1\,0\,\bar{1}\,7)$ and $(\bar{1}\,0\,1\,7)$, lying at 15 and 45°, respectively, to the cracking plane. Thus, hydrides preferentially will precipitate on $(\bar{1}\,0\,1\,7)$, plane due to the higher resolved tensile stress on it, leading to the formation of a slanting crack as shown in Fig. 5(b). Likewise, since L45 specimen has habit planes lying at 30 and 60°, respectively to the notch direction (Table 1), the crack grows only on the habit planes lying at 30° to the notch direction (Table 1), leading to the tilting of the crack as shown in Fig. 2(c). In contrast, L0 specimen has the hydride habit planes tilted $\pm 15°$ to the notch direction $\langle 1\,0\,\bar{1}\,0\rangle$ as shown in Fig. 5(c). Since the precipitation of hydrides is more probable only on one of them, the crack will grow along the plane away from the notch, but will return toward the centerline of the initial notch plane due to the applied tensile stress in the opposite direction. Thus, when the crack is examined minutely, the crack grows in a zig-zag motion with small branching of the crack as shown in Fig. 6 [13]. However, on a macroscopic scale,

Table 1
Growth pattern of a DHC crack on a CT specimen with a notch tilted at various angles to the longitudinal direction

CT specimens	Angle between the notch direction and longitudinal direction (°)	Tilting angle of the grown crack to the notch direction (°)	Tilting angle of the grown crack to the longitudinal direction (°)
L0	0	0	0
L30	30	18	12
L45	45	30	15
L90	90	75	15

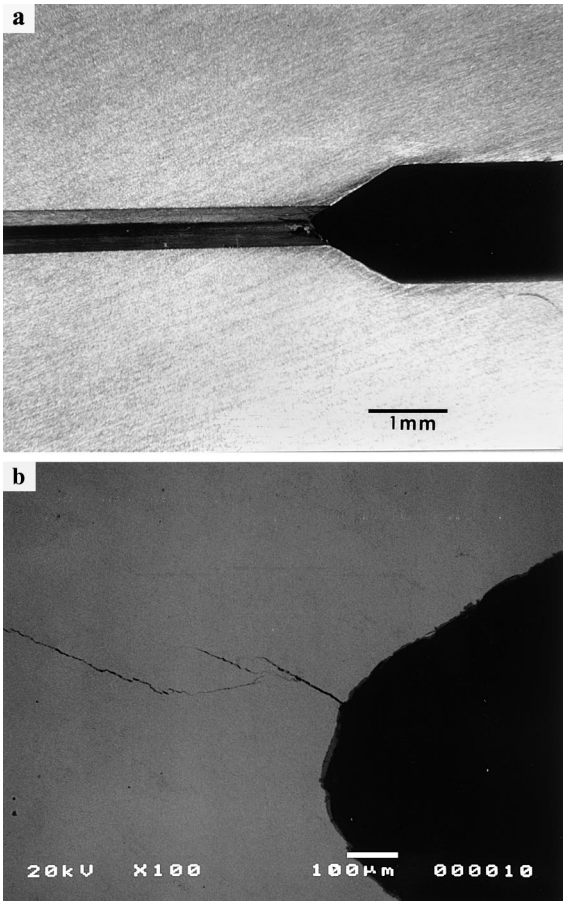

Fig. 3. (a) U type groove formed on both sides of L30 specimen before the initiation of DHC and (b) the slanted crack growth after DHC.

the crack will likely grow parallel to the notch direction as shown in Fig. 2.

In summary, these results demonstrate that the DHC occurs by the fracturing of hydrides precipitated on the habit planes $\{10\bar{1}7\}$ and the resistance of DHC increases with an increasing angle of the hydride habit plane to the notch direction. The threshold stress intensity factor, K_{IH}, required for the initiation of DHC, therefore, would be affected by the slanting angle of the habit planes to the notch direction.

K_{IH} was determined for L0 and L90 CT specimens by plotting the measured crack velocity as a function of stress intensity factor as shown in Fig. 7. As expected, L0 CT specimen, where the hydride habit planes are lying almost parallel to the notch direction, had a quite low K_{IH} of around 5.5 MPa $\sqrt{m}$ while L90 specimen showed a much higher K_{IH} of 18 MPa $\sqrt{m}$. Likewise, Coleman [11] also reported a large threshold stress intensity factor, K_{IH}, of about 15 MPa $\sqrt{m}$ on the CT specimen with a crack propagating into the circumferential direction of the tube. Therefore, a difference in the threshold stress intensity factor between L0 and L90 specimens is concluded to be related to the angle of the

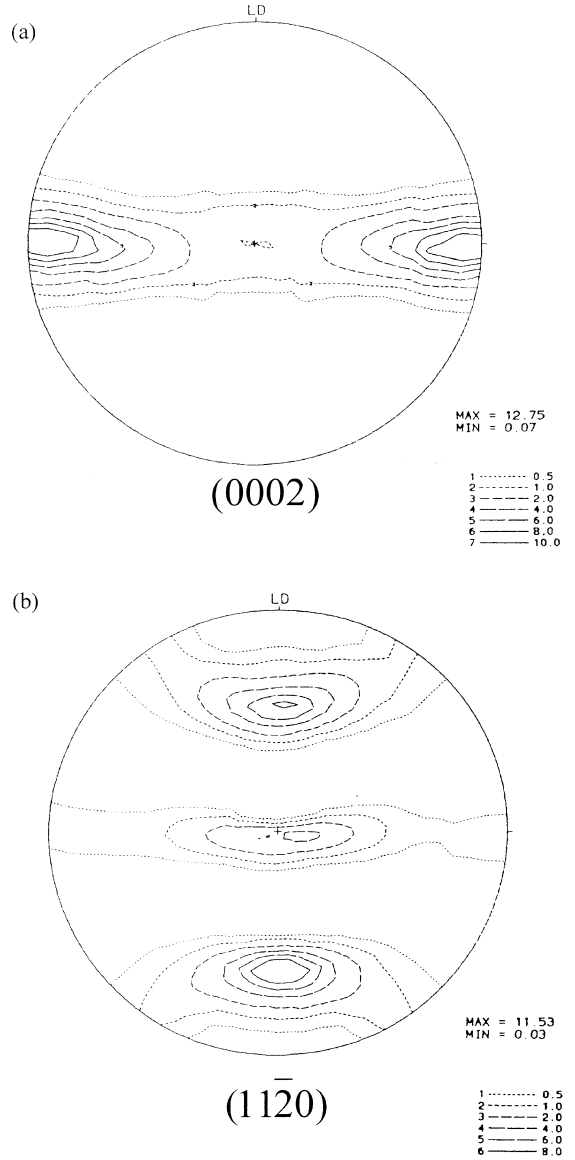

Fig. 4. (0002) and (11$\bar{2}$0) texture of the Zr–2.5Nb pressure tube used.

Table 2
Basal pole components of Zr–2.5Nb pressure tube

Material	Basal pole components		
	Radial, f_r	Transverse, f_t	Longitudinal, f_l
Zr–2.5Nb pressure tube	0.33	0.60	0.07

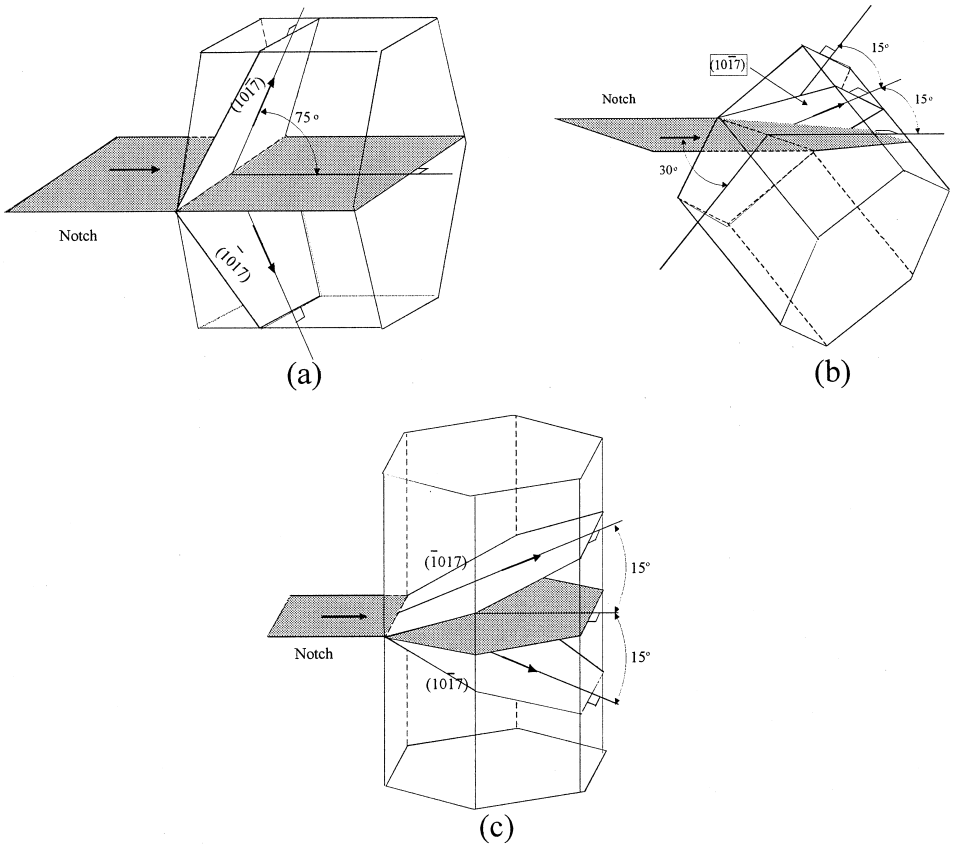

Fig. 5. Relationship between the notch and $\{10\bar{1}7\}$ hydride habit planes for: (a) L90; (b) L30 and (c) L90 specimens.

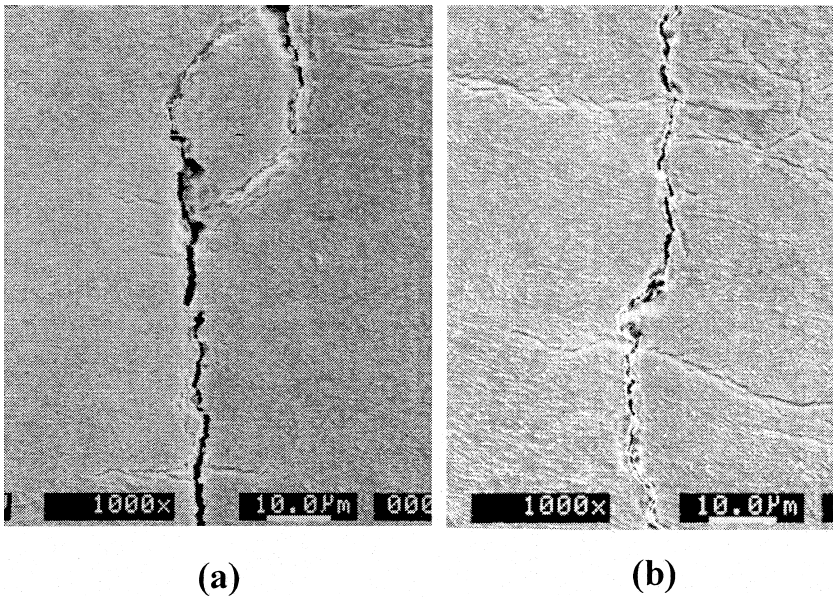

Fig. 6. (a) Small branching and (b) zig-zag pattern of the crack on L0 specimen.

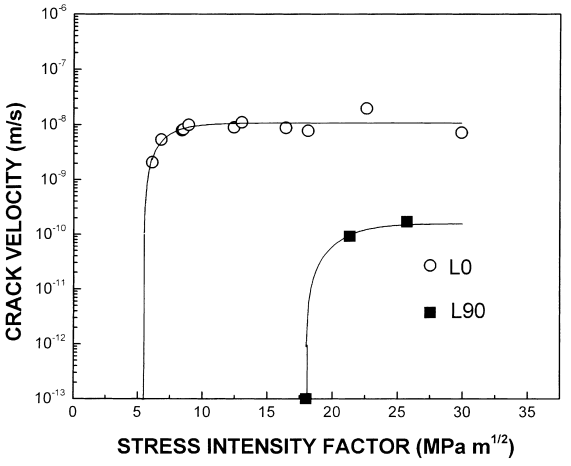

Fig. 7. Crack velocity as a function of stress intensity factor for L0 and L90 specimens.

hydride habit plane and the cracking plane (notch plane). In other words, the threshold stress intensity factor strongly depends on how many habit planes are present along the cracking plane.

To explain the effect of the angle between the hydride habit plane and the cracking plane on the threshold stress intensity factor, the hydride fracture criterion by Shi and Puls [14] is introduced. Here, we assume a single hydride platelet at the crack tip that is inclined at θ to the notch direction as shown in Fig. 8. The local stress applied to the hydride platelet, σ_{loc} is the sum of the stress component normal to the habit plane, $\sigma_{\theta\theta}$ and a stress within the hydride, σ^{h}, generated by the hydride formation process due to its misfit strain with no external stress. The threshold condition is achieved if the local stress is equal to the stress needed for hydride fracture, $\sigma_{\text{f}}^{\text{h}}$. Since $\sigma_{\text{f}}^{\text{h}}$ is constant material property, independent of the inclination angle, θ and σ^{h} is also

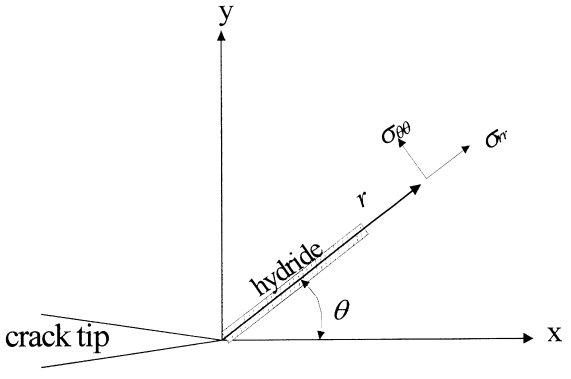

Fig. 8. Hydride platelet precipitated with an angle, θ to the notch direction at the notch tip and the resolved normal stress applied on it.

constant, $\sigma_{\theta\theta}$ must be constant at the initiation of DHC. The normal component of the crack tip stress at an inclined crack is given at the plain stress condition by [15]

$$\sigma_{\theta\theta} = \frac{K_{\text{I}}}{\sqrt{2\pi r}}\left(\frac{3}{4}\cos\left(\frac{\theta}{2}\right) + \frac{1}{4}\cos\left(\frac{3\theta}{2}\right)\right). \tag{1}$$

Therefore, at the threshold condition for the DHC initiation, K_{IH} is approximately given by

$$K_{\text{IH}} = \frac{\sigma_{\text{f}}^{\text{h}}\sqrt{2\pi r}}{[(3/4)\cos(\theta/2) + (1/4)\cos(3\theta/2)]} = \sigma_{\text{f}}^{\text{h}}\sqrt{2\pi r} f(\theta), \tag{2}$$

where K_{IH} is the threshold stress intensity factor depending on the angle, θ and $f(\theta) = [(3/4)\cos(\theta/2) + (1/4)\cos(3\theta/2)]^{-1}$. The ratio of the K_{IH} of L0 and L90 specimens can be calculated as such:

$$K_{\text{IH at } \theta=75^\circ}/\text{K}_{\text{IH at } \theta=15^\circ} = 1.95.$$

This calculated ratio seems to differ from the measured ratio of the K_{IH} for L0 and L90 specimens, 3.3. However, considering that the K_{IH} of L0 CT specimens were in the range of 4.3–12 MPa $\sqrt{\text{m}}$ (the averaged value of 8–9 MPa $\sqrt{\text{m}}$ [14], therefore, the measured K_{IH} of 18 MPa $\sqrt{\text{m}}$ for L90 CT specimens looks quite reasonable.

3.2. Dependence of K_{IH} on texture

Eq. (2) suggests that K_{IH} would decrease with an increasing number of habit planes on the cracking plane, from the maximum values of K_{IH} at the angle θ of 90°.

Therefore, since the habit planes are almost parallel to the basal planes, Eq. (2) can be described more explicitly as such:

$$K_{\text{IH}} = K_{\text{IH at } \theta=90^\circ} - cF_{\text{CP}}, \tag{3}$$

where c is constant and F_{CP} is a basal pole component in the cracking plane defined by Eq. (4):

$$F_{\text{CP}} = \sum V_a \cos^2\alpha. \tag{4}$$

Here, α is the angle between the basal pole of the grain and the direction of interest and V is the volume fraction of grains tilted at an angle α. When the notch grows into the longitudinal direction of the tube or the rolling direction of the plate, F_{CP} must be the basal pole components in the circumferential direction. To systematically demonstrate the texture effect on K_{IH}, Zr–2.5Nb plates were subjected to rolling and cross rolling to change the basal pole components as shown in Table 3. CT specimens that were charged electrolytically with 200 ppm hydrogen followed by annealing at 367°C for 1h were subjected to DHC testing at 200°C. More detailed experimental procedures are described in the paper reported by Kim et al. [16]. The threshold stress intensity factors of Zr–2.5Nb plates were plotted as a

Table 3
Basal pole components of Zr–2.5Nb plates used for the K_{IH} determination [13]

Materials		Basal pole components		
		Normal	Transverse	Longitudinal
Zr–2.5Nb plate A	As-received	0.42	0.54	0.04
	30% Cross rolled	0.54	0.39	0.07
	30% Direct rolled	0.41	0.53	0.06
Zr–2.5Nb plate B	As-received	0.66	0.19	0.15
	30% Cross rolled	0.71	0.14	0.15
	30% Direct rolled	0.69	0.18	0.15

function of the basal pole component, F_{CP} in the cracking plane as shown in Fig. 9 along with the reported K_{IH} from Coleman [11,17], Hwang [12] and Mills [18]. As expected, K_{IH} decreased linearly with an increase in the basal pole component as such:

$$K_{IH} = 17.1 - 17F_{CP}. \quad (5)$$

In other words, the higher the number of habit planes in the cracking plane, the lower the threshold stress intensity factor, K_{IH}. By introducing the basal component of L90 specimen, 0.7 into Eq. (5), the threshold stress intensity factor of L90 specimen is calculated to be 16 MPa $\sqrt{m}$. This calculated K_{IH} seems to comparatively agree well with the measured K_{IH} of the L90 specimen, 18 MPa $\sqrt{m}$, considering a difference in the measured K_{IH} data reported by this study and Coleman [11]. Thus, a conclusion is drawn that the threshold stress intensity factor, K_{IH} decreases linearly with an increasing number of the hydride habit planes $\{10\bar{1}7\}$ in the cracking plane.

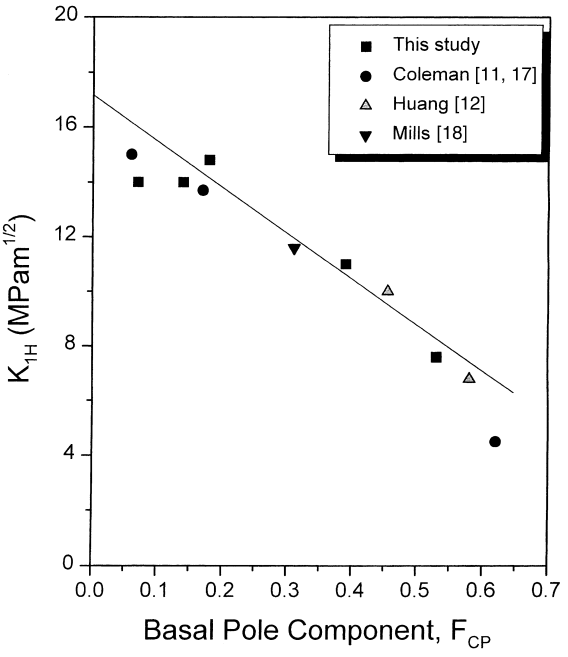

Fig. 9. Threshold stress intensity factor of Zr–2.5Nb plates with basal pole components in the cracking plane.

4. Conclusion

A crack in Zr–2.5Nb pressure tube grew by the fracturing of hydrides along the hydride habit planes, leading to the appearance of a slanted crack growth or crack branching when the cracking plane was tilted at some angles, 30–90°, to the habit planes. Consequently, the threshold stress intensity factor, K_{IH} depends on the angle of hydride habit plane $\{10\bar{1}7\}$ and the cracking plane: $K_{IH} = 5.5$ MPa $\sqrt{m}$ when the cracking plane is parallel to the basal plane or at 15° to the habit plane $\{10\bar{1}7\}$, $K_{IH} = 18$ MPa $\sqrt{m}$ when the cracking plane is normal to the basal plane or at 75° to the habit plane $\{10\bar{1}7\}$.

A supplementary experiment was carried out additionally to demonstrate that K_{IH} decreases linearly with an increasing basal component factor in the cracking plane. Thus, it is concluded that the initiation of DHC is determined by the nucleation rate of hydride precipitates on the habit planes $\{10\bar{1}7\}$ at the crack tip. Furthermore, the DHC resistance of Zr–2.5Nb pressure tubes can be increased by controlling the texture.

Acknowledgements

This work has been carried out as a PHWR Pressure Tube Material Project of the Nuclear R&D program supported by the Ministry of Science and Technology.

References

[1] K.S. Choi, Development of regulatory guideline for the pressure tube integrity of domestic CANDU reactors, Korea Institute of Nuclear Safety Report KINS/AR-122, 1991.

[2] B.A. Cheadle, E.G. Price, Operating performance of CANDU pressure tubes, Atomic Energy of Canada Limited Report AECL-9939, 1989.
[3] C.E. Coleman, J.F.R. Ambler, Zirconium in the Nuclear Industry, ASTM STP 633, American Society for Testing and Materials, 1977, p. 589.
[4] K. Nuttall, A.J. Rogowski, J. Nucl. Mater. 80 (1979) 279.
[5] B.A. Cheadle, C.E. Coleman, J.F.R. Ambler, in: Proceedings of the Sixth International Symposium on Zirconium in the Nuclear Industry, ASTM STP 939, 1987, p. 224.
[6] D.G. Westlake, J. Nucl. Mater. 26 (1968) 208.
[7] Young Suk Kim et al., Development of Zr–Nb alloys for pressure tubes, Korea Atomic Energy Research Institute Report KAERI/RR-1523/94, 1995.
[8] J.Y. Oh, MS thesis, Korea Advanced Institute of Science and Technology, 1995.
[9] S. Sagat, C.E. Coleman, M. Griffiths, B.J.S. Wilkins, in: Proceedings of the 10th International Symposium on Zirconium in the Nuclear Industry, ASTM STP 1245, 1994, p. 35.
[10] V. Perovic, G.C. Weatherly, C.J. Simpson, Acta Metall. 31 (1983) 1381.
[11] C.E. Coleman, in: Proceedings of the Fifth Conference on Zirconinum in the Nuclear Industry, ASTM STP 754, 1982, p. 393.
[12] F.H. Huang, W.J. Mills, Metall. Trans. 22A (1991) 2049.
[13] Y.S. Kim, S.M. Seon, S.S. Kim, S.I. Kwun, J. Korean Inst. Met. Mater. 38 (2000) 35.
[14] S.Q. Shi, M.P. Puls, J. Nucl. Mater. 208 (1994) 232.
[15] T.L. Anderson, Fracture Mechanics: Fundamentals and Applications, CRC, Boca Raton, FL, 1995.
[16] S.S. Kim, S.C. Kim, Y.S. Kim, J. Nucl. Mater. 273 (1999) 52.
[17] C.E. Coleman, S. Sagat, K.F. Amouzouvi, Control of microstructure to increase the tolerance of zirconium alloys to hydride cracking, Atomic Energy of Canada Limited Report AECL-9524, 1987.
[18] W.J. Mills, F.H. Huang, Eng. Frac. Mech. 39 (1991) 241.